1521-0111/86/6/760–772$25.00
MOLECULAR PHARMACOLOGY

http://dx.doi.org/10.1124/mol.114.095505
Mol Pharmacol 86:760–772, December 2014

Potentiation of High Voltage–Activated Calcium Channels by 4-Aminopyridine Depends on Subunit Composition

Li Li, De-Pei Li, Shao-Rui Chen, Jinjun Chen, Hongzhen Hu, and Hui-Lin Pan

Center for Neuroscience and Pain Research (L.L., D.-P.L, S.-R.C., J.C., H.-L.P.), Department of Anesthesiology and Perioperative Medicine, The University of Texas MD Anderson Cancer Center, Houston, Texas; College of Bioscience and Biotechnology (J.C.), Hunan Agricultural University, Changsha, P.R. China; and Department of Integrative Biology and Pharmacology (H.H.), The University of Texas Medical School, Houston, Texas

Received August 21, 2014; accepted September 26, 2014

ABSTRACT

4-Aminopyridine (4-AP, fampridine) is used clinically to improve neuromuscular function in patients with multiple sclerosis, spinal cord injury, and myasthenia gravis. 4-AP can increase neuromuscular and synaptic transmission by directly stimulating high voltage–activated (HVA) Ca^{2+} channels independent of its blocking effect on voltage-activated K^+ channels. Here we provide new evidence that the potentiating effect of 4-AP on HVA Ca^{2+} channels depends on the specific combination of voltage-activated calcium channel $\alpha 1$ ($Cav\alpha_1$) and voltage-activated calcium channel β ($Cav\beta$) subunits. Among the four $Cav\beta$ subunits examined, $Cav\beta 3$ was the most significant subunit involved in the 4-AP–induced potentiation of both L-type and N-type currents. Of particular note, 4-AP at micromolar concentrations selectively potentiated L-type currents reconstituted with Cav1.2, $\alpha_2\delta 1$, and $Cav\beta 3$. In contrast, 4-AP potentiated N-type currents only at much higher concentrations and had little effect on P/Q-type currents. In a phrenic nerve–diaphragm preparation, blocking L-type Ca^{2+} channels eliminated the potentiating effect of low concentrations of 4-AP on end-plate potentials. Furthermore, 4-AP enhanced the physical interaction of Cav1.2 and Cav2.2 subunits to $Cav\beta 3$ and also increased their trafficking to the plasma membrane. Site-directed mutagenesis identified specific regions in the guanylate kinase, HOOK, and C-terminus domains of the $Cav\beta 3$ subunit crucial to the ability of 4-AP to potentiate L-type and N-type currents. Our findings indicate that 4-AP potentiates HVA Ca^{2+} channels by enhancing reciprocal Cav1.2-$Cav\beta 3$ and Cav2.2-$Cav\beta 3$ interactions. The therapeutic effect of 4-AP on neuromuscular function is probably mediated by its actions on $Cav\beta 3$-containing L-type Ca^{2+} channels.

Introduction

Voltage-activated Ca^{2+} channels are critically involved in many physiologic functions, including neurotransmitter and hormone release, cell excitability, muscle contraction, and gene transcription (Catterall, 2000; Catterall and Few, 2008). According to their activation voltage, Ca^{2+} channels can be generally divided into three major classes: 1) high voltage–activated (HVA) Ca^{2+} channels, which include P/Q-type, N-type, and L-type; 2) intermediate voltage–activated R-type; and 3) low voltage–activated T-type (Cav3) (Catterall, 2000; Catterall et al., 2005). 4-Aminopyridine (4-AP, fampridine) is used clinically to treat neuromuscular dysfunction in several disease conditions, including multiple sclerosis (Davis et al., 1990), spinal cord injury (Hansebout et al., 1993), myasthenia gravis (Lundh et al., 1979), Lambert-Eaton syndrome (Kim and Neher, 1988; Giovannini et al., 2002), and episodic ataxia type 2 (Strupp et al., 2004). Although 4-AP has long been considered a voltage-activated K^+ channel blocker, we have recently shown that it can directly stimulate both native and cloned HVA Ca^{2+} channels (but not low voltage–activated Ca^{2+} channels) to elicit neurotransmitter release without involvement of voltage-activated K^+ channels (Wu et al., 2009). However, the molecular mechanisms underlying potentiation of the HVA Ca^{2+} channels by 4-AP have yet to be defined.

HVA Ca^{2+} channels are plasma membrane–bound protein complexes typically composed of α_1, $\alpha_2\delta$, and β subunits (Catterall, 2000; Catterall et al., 2005). The HVA α_1 subunit proteins ($Cav\alpha_1$) are divided into two major subfamilies, Cav1 and Cav2, on the basis of amino acid sequence similarity. The Cav1 subfamily consists of four types, Cav1.1–1.4, all of which encode L-type Ca^{2+} channels. The Cav2 subfamily consists of three types, Cav2.1, Cav2.2, and Cav2.3, which encode P/Q-type, N-type, and R-type Ca^{2+} channels, respectively. The $Cav\alpha_1$ subunits contain the channel pore and voltage sensor and are the main determinant of biophysical and pharmacological characteristics, whereas the cytosolic β subunits ($Cav\beta$) play essential roles in regulating the surface expression and stability of HVA $Cav\alpha_1$ subunits (De Waard et al., 1994; Pragnell et al., 1994; Yamaguchi et al., 1998). $Cav\beta$ subunits also contribute to channel gating and second-messenger–dependent modulation of HVA Ca^{2+} channels (Stea et al., 1995; Bourinet et al., 1996; Altier et al., 2011; Waithe et al., 2011; Dolphin, 2012). The four mammalian $Cav\beta$ subunits, $Cav\beta 1$-4, are encoded by different genes and are differentially expressed in various tissues and cell types (Buraei and Yang, 2010). Although we have reported that $Cav\beta 3$ subunit mediates the potentiating

This work was supported by grants from the National Institutes of Health [R01-HL077400 and R01-NS073935] and by the N.G. and Helen T. Hawkins endowment (to H.-L.P.).
dx.doi.org/10.1124/mol.114.095505.

ABBREVIATIONS: 4-AP, 4-Aminopyridine; AID, α-interaction domain; EPPs, end-plate potentials; GFP, green fluorescent protein; GK, guanylate kinase; HEK, human embryonic kidney; HVA, high voltage–activated; Ni-NTA, nickel-nitrilotriacetic acid; SH3, Src homology 3.

effect of 4-AP on the N-type Ca^{2+} channel (Wu et al., 2009), it is unclear whether all Cavα_1 and Cavβ channel complexes are equally affected by 4-AP. Related to these unknowns, 4-AP was found to enhance synaptic and neuromuscular transmission at micromolar concentrations, whereas millimolar concentrations of 4-AP were required to inhibit voltage-activated K^+ channels or stimulate native Ca^{2+} currents (Wu et al., 2009). Further, clinical studies have shown that millimolar concentrations of 4-AP are toxic and irrelevant to its therapeutic effects in humans (Bever et al., 1994; Smith et al., 2000). Thus, it is important to identify the exact Ca^{2+} channel complexes that are sensitive to micromolar concentrations of 4-AP.

In this study, we determined whether the potentiating effect of 4-AP on HVA Ca^{2+} channels is dependent on specific Cavα_1 and Cavβ subunits. We show that 4-AP enhances N-type and L-type currents mainly through the Cavβ3 subunit. Interestingly, at micromolar concentrations, 4-AP selectively potentiates L-type currents. 4-AP appears to act through enhancing the association of Cavβ3 with Cav1.2 and Cav2.2 subunits to increase their trafficking to the plasma membrane. We also identified several regions in the guanylate kinase (GK), HOOK, and C-terminus domains of Cavβ3 that are required for the 4-AP–induced potentiation of N-type and L-type currents. Our findings suggest that the therapeutic action of 4-AP is probably mediated by its effect on L-type Ca^{2+} channels. By acting primarily on the Cavβ3 subunit, 4-AP promotes reciprocal Cav1.2-Cavβ3 and Cav2.2-Cavβ3 interactions to augment channel activity. This new information greatly improves our understanding of the clinically relevant therapeutic action of 4-AP and the molecular mechanisms involved in this action.

Materials and Methods

Cell Culture and Transfection. Human embryonic kidney (HEK) 293A cells, a subclone of the HEK293 cell line, were cultured in Dulbecco's modified Eagle's medium (Gibco/Life Technologies, Grand Island, NY) supplemented with 10% fetal bovine serum (Sigma-Aldrich, St. Louis, MO) at 37°C in a 5% CO_2 incubator. For transfection experiments, 1.2×10^4 cells were plated on poly-L-lysine–coated cover slips in each well of a 24-well-plate. After 24 hours, we used PolyJet DNA In Vitro Transfection Reagent (SigaGen Laboratories, Gaithersburg, MD) to transiently transfect the cells with various combinations of Cavα_1 (Cav1.2, Cav2.1, and Cav2.2), $\alpha_2\delta$1, and Cavβ (Cavβ1-4) subunits. The cDNAs for rat Cav1.2, Cavβ1, Cavβ2a, and Cavβ4 were as previously described (Stea et al., 1995; Bourinet et al., 1996); the rat green fluorescent protein (GFP)–tagged Cav2.2 cDNA was provided by Dr. Tsutomu Tanabe (Tokyo Medical and Dental University); and cDNAs for rat Histidine-tagged Cav2.2 (His-Cav2.2), Cavβ3, and $\alpha_2\delta$1 were kindly provided by Dr. Diane Lipscombe (Brown University). To construct GFP-Cavβ3, we inserted a 1.5-kb EcoRI-BamHI fragment from Cavβ3 into the expression vector pEGFP-C1 (Clontech, Mountain View, CA). To construct His-Cav1.2, a 6906-base pair NotI-HindIII fragment from Cav1.2 was inserted into the expression vector pcDNA6/V5-His ABC (Invitrogen/Life Technologies). We cotransfected HEK293A cells with multiplasmids of HVA Ca^{2+} channels at 1:1:1 ratio and replaced the culture medium with new medium after 4 hours. Electrophysiological recordings and biochemical assays were performed 48 hours after transfection.

Electrophysiological Recording. Whole-cell currents were recorded using barium as the charge carrier (I_{Ba}) as described previously (Wu et al., 2009; Li et al., 2012). Recording electrodes (resistance, 2–3 MΩ) were pulled from glass capillaries and fire-polished. The extracellular recording solution consisted of (in mM) 140 TEA, 2 $MgCl_2$, 3 $BaCl_2$, 10 glucose, and 10 HEPES (pH 7.4; osmolarity, 320 mOsm). The pipette solution consisted of (in millimolar) 120 CsCl, 1 $MgCl_2$, 10 HEPES, 10 EGTA, 4 MgATP, and 0.3 NaGTP (pH 7.2; osmolarity, 300 mOsm). Whole-cell currents were recorded with an EPC-10 amplifier (HEKA Instruments, Lambrecht, Germany) from a holding potential of –90 mV to a test potential of 0 mV. Signals were filtered at 1 kHz, digitized at 10 kHz, and acquired using the Pulse program (HEKA Instruments). After the whole-cell configuration was established, the cell membrane capacitance and series resistance were electronically compensated. The Ca^{2+} channel voltage-dependent inactivation was assessed by depolarizing cells with a series of prepulse potentials from –90 to 10 mV for 500 milliseconds followed by a command potential to 0 mV for 150 milliseconds (Wu et al., 2009; Li et al., 2012). All experiments were performed at room temperature (~25°C).

Cavα_1-Cavβ3 Association Assays. HEK293A cells were transfected with $\alpha_2\delta$1 and GFP-Cavβ3 plus either His-Cav2.2 or His-Cav1.2 when cells were grown to 85% confluence in 75 cm^2 culture flasks. After 48 hours, cells were treated with 4-AP for 5 minutes and quickly collected using a 25-cm scraper (Sarstedt Inc., Newton, NC) and pelleted by centrifugation at 1500 rpm for 3 minutes at 4°C. All steps were performed in medium including 4-AP and completed within 10 minutes. Cells treated with DMEM (without 4-AP) were used as a negative control. Because Cav1.2 and Cav2.2 were tagged with 6×His, we used the nickel-nitrilotriacetic acid (Ni-NTA, for purification of 6×His-containing recombinant proteins) system (Invitrogen/Life Technologies, Grand Island, NY) to determine the amount of 4-AP–induced Cavα_1-Cavβ3 binding. In brief, we used sonication buffer (0.5 M NaCl, 50 mM NaH_2PO_4, and 10 mM imidazole, pH 8.0) containing protease inhibitors (Sigma-Aldrich) to extract total proteins from transfected cells. We then used gentle rotation to mix the protein with Ni-NTA resin at 4°C. After 1 hour, the proteins were filtered through a Ni-NTA agarose column and washed three times by gravity in the wash buffer (0.5 M NaCl, 50 mM NaH_2PO_4, and 20 mM imidazole, pH 8.0). Finally, the proteins were obtained with the elution buffer (0.5 M NaCl, 50 mM NaH_2PO_4, and 250 mM imidazole, pH 8.0). To quantify the eluted Cavβ3 proteins, we performed Western blot analysis using an anti-Cavβ3 antibody (1:1,000 dilution; Santa Cruz Biotechnology, Dallas, TX).

A fluorescence spectrophotometer (SpectraMax; Molecular Devices, Sunnyvale, CA) was also used to quantify the eluted proteins by taking advantage of GFP-tagging of the Cavβ3 construct. The GFP-Cavβ3 proteins were excited at 430 nm, and fluorescence emission was detected at 509 nm. The relative fluorescence unit of GFP-Cavβ3 from 4-AP–treated cells was normalized to cells that were not treated with 4-AP. The mean value of relative fluorescence unit of cells that were not treated with 4-AP was defined as 1.

Western Blot Analysis of Plasma Membrane Cavα_1 Proteins. HEK293A cells cotransfected with Cav1.2 (or GFP-Cav2.2), $\alpha_2\delta$1, and Cavβ3 (or Cavβ2) were sonicated in RIPA buffer (Cell Signaling Technology, Danvers, MA) in the presence of a cocktail of protease inhibitors (Sigma-Aldrich). Total proteins were obtained by centrifugation at 16,000*g* for 10 minutes at 4°C. To extract the plasma membrane protein, we used the ProteoExtract subcellular proteome extraction kit (Calbiochem; EMD Millipore, Billerica, MA) according to the manufacturer's instructions. In brief, cells were incubated in 1 ml extraction buffer I and then shaken for 10 minutes at 4°C. The extraction buffer I including the cytosolic protein was then collected and incubated with 1 ml extraction buffer II, containing protease inhibitors, for 30 minutes at 4°C. After the extraction buffer II containing membrane proteins was collected, 30 μg of protein was subjected to SDS-PAGE and transferred onto a polyvinylidene difluoride membrane (Immobilon P; EMD Millipore). Blots were probed with either anti-Cav1.2 antibody (1:1000 dilution; NeuroMab/UC Davis) or anti-GFP antibody (1:1000 dilution; Santa Cruz Biotechnology). Anti-GAPDH antibody (1:1,000 dilution; EMD Millipore) was used as a loading control and for normalization. The ImageJ software program was used to quantify the protein band intensities. The amounts of GFP-Cav2.2 and Cav1.2 proteins were normalized to GAPDH. The mean value of cells that were not treated with 4-AP was defined as 1.

Cell Surface Protein Isolation and Cav1.2 Trafficking. HEK293A cells transfected with Cav1.2, $\alpha 2\delta$1, and GFP-Cavβ3 were

treated with 4-AP for 5 minutes and quickly washed twice with phosphate-buffered saline. Cell surface biotinylation was carried out using the Cell Surface Protein Isolation Kit (Pierce Biotechnology, Rockford, IL) following manufacturer's instructions. Briefly, cells were incubated with sulfo-NHS-SS-biotin that covalently binds to primary amino groups of extracellular proteins at 4°C with constant rotation for 30 minutes. Excess biotin was quenched with quenching solution. The cells were washed, harvested through gentle scraping, and lysed using the lysis buffer in the presence of a protease inhibitor cocktail (Sigma-Aldrich) for 30 minutes at 4°C. The lysates were centrifuged for 2 minutes at 10,000*g* at 4°C, and the clear supernatants were added to NeutrAvidin agarose and incubated for 60 minutes at 26°C with end-over-end mixing. The unbound (unbiotinylated) proteins, representing the intracellular fraction, were separated from the captured surface proteins by centrifugation of the column. Finally, the captured surface proteins were eluted from the biotin–NeutrAvidin Agarose by incubation with dithiothreitol in SDS-PAGE sample buffer and subjected to Western blot analysis using Cav1.2 antibody. The intracellular fraction containing GAPDH was used as an internal loading control.

Site-Directed Mutagenesis. Point mutation and insertion in Cavβ3 were performed using the QuikChange II XL Site-Directed Mutagenesis Kit (Stratagene/Agilent Technologies, Santa Clara, CA). Overlap extension polymerase chain reaction was used to perform domain swap between Cavβ3 and Cavβ2 at the equivalent position for the Cavβ3-P1 domain. The primers used for Cavβ3-P1 domain swap were GGCTCAAACAGGAACAGAAGGCCAAGCAAGGG and GGAGGAGGGGAACGTCGGTTACTGGGTAC TATGTCACC.

End-Plate Potential Recording. To determine whether L-type channels mediate the potentiating effect of 4-AP on the neuromuscular transmission, we recorded end-plate potentials (EPPs) using a phrenic nerve–diaphragm preparation (Wu et al., 2009). Briefly, male Sprague-Dawley rats weighing 120–150 g were anesthetized with isoflurane, and the diaphragm and attached phrenic nerve were removed rapidly and pinned in a 35-mm Sylgard-lined petri dish. The tissue was superfused with oxygenated Ringer's solution containing (in millimolar) 116 NaCl, 5 KCl, 2 $CaCl_2$, 1 $MgSO_4$, 1 NaH_2PO_4, 23 $NaHCO_3$, and 11 glucose (pH 7.2–7.3) and continuously gassed with 95% O_2 and 5% CO_2. Muscle contraction was selectively blocked with 2.3 μM μ-conotoxin GIIIB, which preferentially blocks voltage-activated Na^+ channels in the skeletal muscle. Intracellular recording was performed by using a glass sharp-electrode (5–15 MΩ filled with 3 mM KCl) at 25°C. The electrode was inserted into the diaphragm by using a micromanipulator until the EPPs of muscle fibers were recorded. EPPs were evoked with supramaximal electrical stimuli applied to the phrenic nerve (pulse width, 0.2 milliseconds) via a suction electrode. EPP signals were processed with a Multiclamp 700B amplifier (Molecular Devices, Sunnyvale, CA). The areas under the curve of the evoked EPPs were integrated and analyzed before and during 4-AP application.

Data Analysis. Results are expressed as means ± S.E.M. The PulseFit software program (HEKA Instruments) was used to analyze the whole-cell current data. Conductance-voltage (G-V) curves were fit using the Boltzmann equation,

$$G/G_{max} = \frac{1}{1 + \exp(V_{0.5} - \frac{Vm}{k})}$$

in which $V_{0.5}$ is the voltage for 50% activation or inactivation and k is a voltage-dependent slope factor. Student's t test was used to compare differences between two groups. One-way analysis of variance with Dunnett's post-hoc test was used to compare differences among more than two groups (i.e., the concentration-dependent effect of 4-AP). $P < 0.05$ was considered to be statistically significant.

Results

4-AP Differentially Potentiates L-Type and N-Type, but Not P/Q-Type, Currents. We previously reported that 4-AP rapidly and reversibly increases N-type whole-cell currents in transfected HEK293 cells (Wu et al., 2009). To determine whether this is a general effect across HVA Ca^{2+} channels, we first compared the dose-response relationship of 4-AP (0.03–3 mM) on L-type (Cav1.2), P/Q-type (Cav2.1), and N-type (Cav2.2) Ca^{2+} channels in HEK293 cells cotransfected with $\alpha_2\delta1$ and Cavβ3 subunits. Cells were voltage-clamped at –90 mV and depolarized to 0 mV for 200 milliseconds. 4-AP rapidly and reversibly increased N-type whole-cell Ba^{2+} currents but only at concentrations >1 mM (Fig. 1). Strikingly, 4-AP significantly increased L-type currents at a concentration as low as 0.1 mM, and its potentiating effect was concentration-dependent (Fig. 1). In contrast, 4-AP had little effect on P/Q-type currents even at 30 times higher (3 mM). These data indicate that the stimulating effect of 4-AP on HVA Ca^{2+} channels is subtype-specific and that at micromolar concentrations, 4-AP selectively potentiates Cav1.2-mediated currents, the major L-type Ca^{2+} channel isoform present in neurons (Hell et al., 1993; Bourinet et al., 1994).

4-AP Potentiates N-Type and L-Type Channels Mainly through Cavβ3. We have shown that the Cavβ3 subunit is essential for the potentiating effect of 4-AP on N-type Ca^{2+} channels (Wu et al., 2009). We next determined whether Cavβ1–β4 are differentially involved in the potentiating effect of 4-AP on different types of HVA Ca^{2+} channels. We cotransfected HEK293 cells with various combinations of individual Cavβ and Cavα_1 subunits all in the presence of the $\alpha_2\delta1$ subunit. Whereas bath application of 0.1–3 mM 4-AP caused a rapid and large increase in L-type whole-cell currents in the presence of Cavβ3 (Fig. 2, A and B), 4-AP at 1–3 mM produced only a small increase in L-type currents when Cavβ3 was replaced with Cavβ2. 4-AP had no effect on L-type currents when Cavβ3 was substituted with Cavβ1 or Cavβ4 (Fig. 2, A and B). Furthermore, 4-AP significantly increased the voltage-dependent activation, but not voltage-dependent inactivation, of L-type currents in the presence of Cavβ3, but not Cavβ2, subunit (Fig. 2, C and D; Table 1).

When the Cav2.2 and $\alpha_2\delta1$ were cotransfected with Cavβ3 or Cavβ4, 4-AP likewise increased whole-cell Ba^{2+} currents at 3–5 mM (Fig. 2, A and B). When Cav2.2 and $\alpha_2\delta1$ were cotransfected with Cavβ1, 3–5 mM 4-AP also increased Ba^{2+}currents, but its effect was smaller than that observed with Cavβ3 or Cavβ4. In contrast, when Cav2.2 and $\alpha_2\delta1$ were cotransfected with Cavβ2, 4-AP at 3–5 mM produced only a small increase in N-type currents, which was also observed in HEK293 cells cotransfected with Cav2.2 and $\alpha_2\delta1$ only (Fig. 2, A and B). 4-AP significantly shifted the voltage-dependent activation of N-type currents in HEK293 cells transfected with the Cavβ3. However, no such shift occurred in cells transfected with Cavβ2 during 4-AP treatment (Fig. 2, C and D; Table 1).

In HEK293 cells transfected with Cav2.1, $\alpha_2\delta1$, and either Cavβ3 or Cavβ4, 4-AP only slightly increased P/Q-type currents even at 5–10 mM (Fig. 2, A and B). 4-AP had no effect on P/Q-type currents when Cav2.1 and $\alpha_2\delta1$ were transfected with either Cavβ1 or Cavβ2 (Fig. 2, A and B). Furthermore, 4-AP failed to significantly shift the voltage-dependent activation and inactivation of P/Q-type currents in cells transfected with Cav2.1, $\alpha_2\delta1$, and any of the Cavβ subunits (Fig. 2, C and D; Table 1). Collectively, these data suggest that the potentiating effect of 4-AP on different HVA Ca^{2+} channels depends on the specific combinations of Cavα_1 and Cavβ subunits. Cavβ3 is the most significant subtype

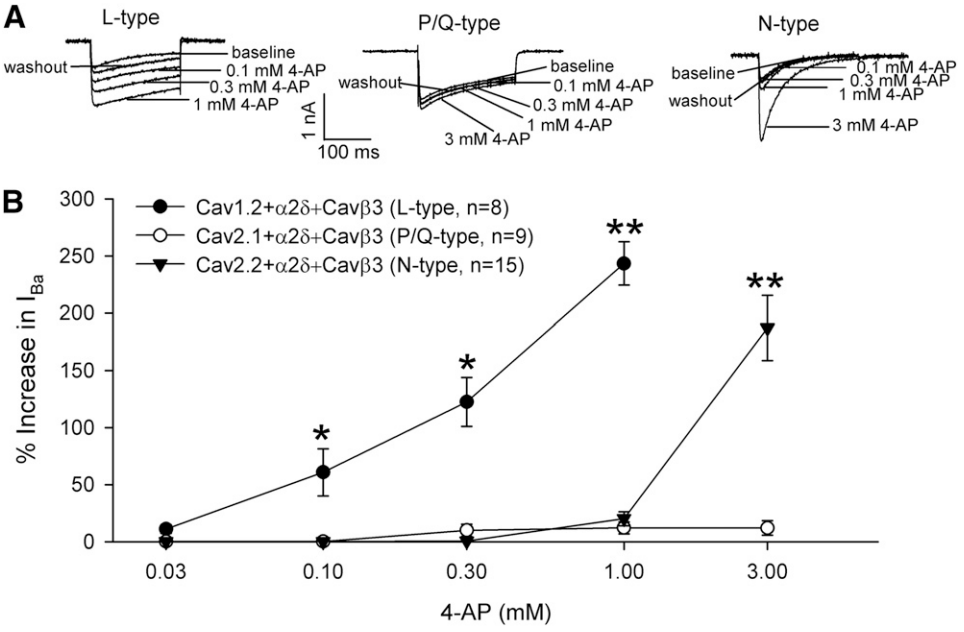

Fig. 1. 4-AP differentially potentiates L-type and N-type, but not P/Q-type, currents. (A) Original current traces show the concentration-dependent effects of 4-AP on L-type (Cav1.2), P/Q -type (Cav2.1), and N-type (Cav2.2) currents in HEK293 cells cotransfected with $\alpha_2\delta1$ and Cav$\beta3$. Ba^{2+} currents (I_{Ba}) were elicited by a test pulse from a holding potential of –90 mV to 0 mV for 200 milliseconds. (B) Concentration-response relationships of 4-AP on L-type, P/Q-type, and N-type currents reconstituted with $\alpha_2\delta1$ and Cav$\beta3$ in HEK293 cells. Note that only the L-type Ca^{2+} channel was potentiated by 4-AP at concentrations <1 mM. $^*P < 0.05$, $^{**}P < 0.01$ compared with respective baseline controls before 4-AP application (repeated measures analysis of variance followed by Dunnett's post hoc test).

involved in the potentiation of L-type and N-type HVA Ca^{2+} channels by 4-AP.

L-Type Channels Contribute to the Potentiating Effect of 4-AP on Neuromuscular Transmission. Motor nerve terminals possess multiple HVA Ca^{2+} channels regulating acetylcholine release (Lin and Lin-Shiau, 1997; Oliveira et al., 2004). We thus used a phrenic nerve–diaphragm preparation to record EPPs to determine whether L-type Ca^{2+} channels are involved in the potentiation of neuromuscular transmission effect by low concentrations of 4-AP. At concentrations of 0.5 and 2 mM, 4-AP significantly increased the amplitude of EPPs in a dose-dependent manner (Fig. 3A). Although nifedipine (10 μM), a selective blocker for L-type Ca^{2+} channels, had no effect on baseline EPPs, it blocked the potentiating effect of 0.5 mM 4-AP on EPPs. On the other hand, 2 mM 4-AP still significantly increased the amplitude of EPPs in the presence of 10 μM nifedipine (Fig. 3B). Bath application of the nonselective HVA Ca^{2+} channel blocker Cd^{2+} (100 μM) abolished EPPs at the end of the experiments. These results indicate that at concentrations <1 mM, 4-AP potentiates EPPs primarily through L-type Ca^{2+} channels.

4-AP Enhances the Interaction of Cav$\beta3$ and Cavα_1 Subunits. To investigate how 4-AP acts to potentiate HVA Ca^{2+} channels through Cav$\beta3$, we examined whether 4-AP influences the binding between Cav$\beta3$ and Cavα_1. We cotransfected HEK293 cells with $\alpha_2\delta1$, GFP-Cav$\beta3$, and His-Cav1.2, and then treated the cells with 4-AP for 5 minutes before protein extraction. Western blot analysis of the eluted fraction from a Ni-NTA affinity column revealed that treatment with 0.3 and 3 mM 4-AP largely increased the amount of Cav$\beta3$ protein retained with Cav1.2 on the column (Fig. 4A). Likewise, 0.3 and 3 mM 4-AP profoundly increased the level of GFP-Cav$\beta3$–Cav1.2 binding in a concentration-dependent manner (Fig. 4B).

In HEK293 cells transfected with $\alpha_2\delta1$, GFP-Cav$\beta3$, and His-Cav2.2, treatment with 3 mM 4-AP also significantly increased the level of Cav$\beta3$ and GFP-Cav$\beta3$ proteins retained with Cav2.2 (Fig. 4, C and D). These results suggest that 4-AP increases or stabilizes Cav$\beta3$ binding to Cav1.2 and Cav2.2 proteins.

4-AP Promotes Plasma Membrane Trafficking of Cav1.2 and Cav2.2. The cytosolic Cavβ subunit plays a major role in the plasma membrane trafficking of the Cavα_1 subunit (Hidalgo et al., 2006). We next determined whether 4-AP acts through Cav$\beta3$ to increase the membrane surface expression of Cavα_1 proteins. In cells cotransfected with $\alpha_2\delta1$, Cav$\beta3$, and Cav1.2, 4-AP (0.3 and 3 mM) elicited a substantial increase in the amount of plasma membrane–bound Cav1.2 protein (Fig. 5A). Likewise, 4-AP (3 mM) also significantly increased the amount of Cav2.2 in the plasma membrane fraction in Cav$\beta3$-transfected cells (Fig. 5C). However, for both L-type and N-type Ca^{2+} channels, 4-AP had no significant effect on the amount of plasma membrane–bound Cav1.2 and Cav2.2 proteins when Cav$\beta3$ was replaced with Cav$\beta2$ (Fig. 5, B and D).

To further ensure that 4-AP promotes the membrane surface expression of Cav$\beta3$–Cav1.2, we used the biotinylation method to isolate cell surface proteins from HEK293 cells transfected with Cav1.2, Cav$\beta3$, and $\alpha_2\delta1$. Treatment with 4-AP (0.3 and 3 mM) for 5 minutes caused a significant increase in the amount of Cav1.2 in membrane surface proteins (Fig. 5E). Collectively, these findings suggest that 4-AP increases Cavα_1 membrane trafficking by acting via a selective interaction with the Cav$\beta3$ subunit.

Identification of Protein Domains of Cav$\beta3$ Responsible for the Distinct Potentiating Effect of 4-AP on Neuronal L-Type and N-Type Channels. The four Cavβ subunits exhibit an overall amino acid sequence identity of about 60%. On the basis of amino acid sequence identity, biochemical, and functional studies, several distinct domains have been identified in the Cavβ subunits (Chen et al., 2004; Opatowsky et al., 2004; Van Petegem et al., 2004). Whereas Src homology 3 (SH3) and GK domains are highly conserved among the four Cavβ subunits, the HOOK region connecting the last two β sheets of the GK domain shows a large difference in amino acid sequence across the four Cavβ subunits (Chen et al., 2004; Buraei and Yang, 2010). Because our findings indicated that 4-AP–induced potentiation of N-type and L-type Ca^{2+} channels is mediated by Cav$\beta3$, but

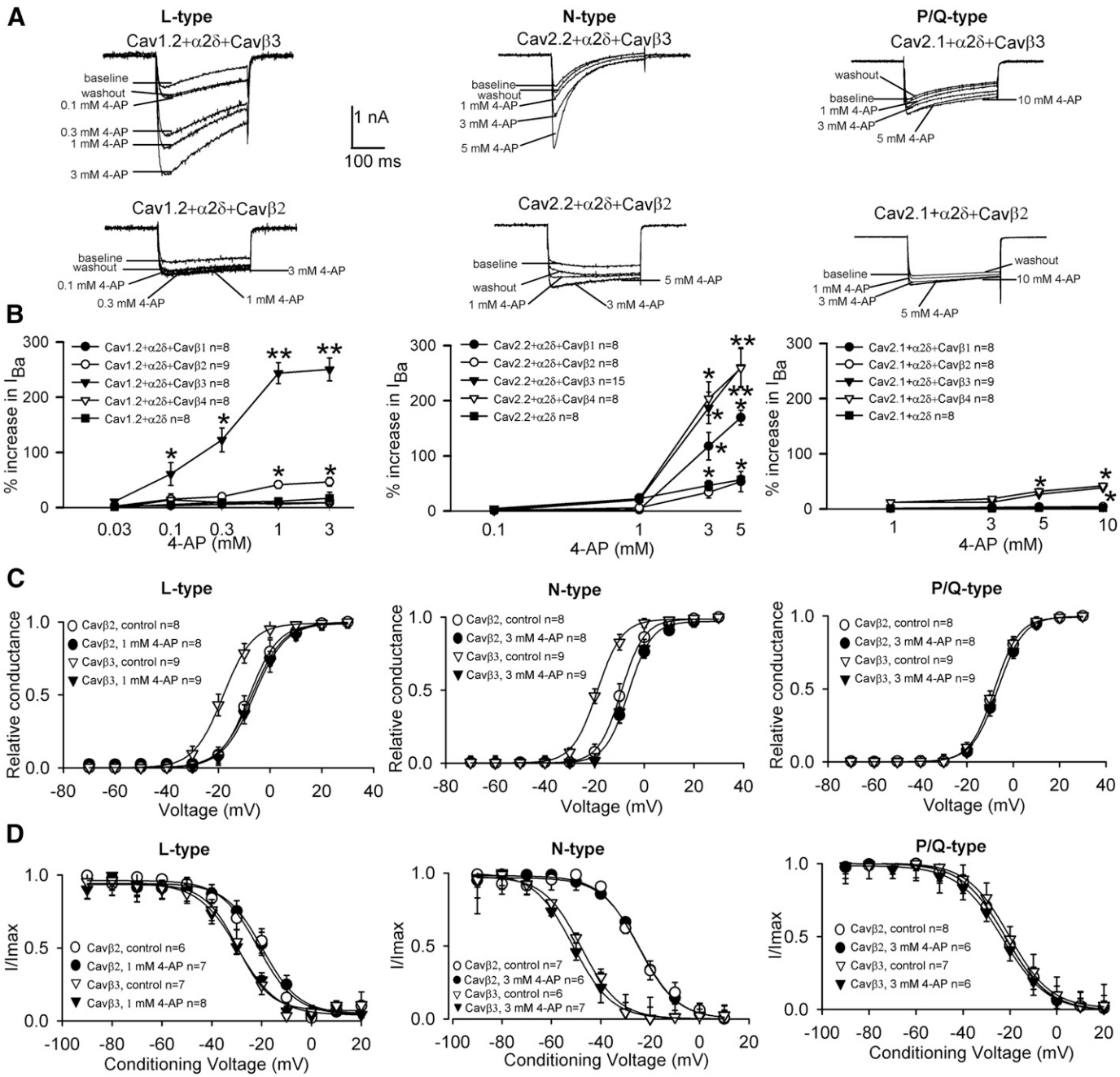

Fig. 2. 4-AP potentiates L-type and N-type currents primarily through Cavβ3. (A) Original current traces show the differential effects of 4-AP on L-type (Cav1.2), N-type (Cav2.2), and P/Q-type (Cav2.1) currents reconstituted with Cavβ3 or Cavβ2 in HEK293 cells (plus $\alpha_2\delta$1). (B) Concentration-response relationships of 4-AP on L-type (Cav1.2), N-type (Cav2.2), and P/Q-type (Cav2.1) currents in HEK293 cells cotransfected with individual Cavβ subunits (plus $\alpha_2\delta$1). Note that micromolar concentrations of 4-AP only potentiated complexes combining Cav1.2 and Cavβ3. (C) Effects of 4-AP on the voltage-dependent activation of L-type, N-type, and P/Q-type Ca^{2+} channels in the presence of Cavβ2 or Cavβ3 (plus $\alpha_2\delta$1). The effects of 4-AP on $V_{0.5}$ and slope factors of L-type, N-type, and P/Q-type currents are listed in Table 1. (D) Effects of 4-AP on the voltage-dependent inactivation of L-type, N-type, and P/Q-type Ca^{2+} channels in the presence of Cavβ2 or Cavβ3 (plus $\alpha_2\delta$1). 4-AP had no significant effects on $V_{0.5}$ and slope factors of L-type, N-type, and P/Q-type currents (see Table 1). $^*P < 0.05$, $^{**}P < 0.01$ compared with the control before 4-AP application (repeated measures analysis of variance followed by Dunnett's post hoc test).

not Cavβ2, we sought to determine whether differences in structural elements between Cavβ3 and Cavβ2 underlie the differential effect of 4-AP. We used site-directed mutagenesis approaches to identify the potential Cavβ3 interaction sites responsible for the 4-AP–induced potentiation of N-type and L-type Ca^{2+} channels. Experimental design and results of the mutagenesis studies are summarized in Fig. 6 and Table 2.

The GK domain of Cavβ is important for interactions with the α-interaction domain (AID) of Cavα_1 (Chen et al., 2004; Van Petegem et al., 2004). We first examined whether the amino acid residues involved in interactions with the AID in the GK domain contribute to the 4-AP–induced potentiation of HVA Ca^{2+} channels. We separated the residues into six groups (A1–A6) and mutated each to alanine (Fig. 6). The A1, A3, A4, and A5 mutants resulted

TABLE 1
Effects of 4-AP on the voltage-dependent activation and inactivation of L-type, N-type, and P/Q-type Ca^{2+} channels in HEK293 cells cotransfected with $\alpha_2\delta1$ and Cav$\beta2$ or Cav$\beta3$
n = 8–10 cells in each group; data are expressed as means ± S.E.M.

	Specific Subunit Combination	$V_{0.5}$	Slope Factor
		mV	*mV*
Voltage-Dependent Activation			
L-type	Cav1.2+$\alpha2\delta1$+Cav$\beta2$ (control)	−6.2 ± 0.1	7.0 ± 0.1
	Cav1.2+$\alpha_2\delta1$+Cav$\beta2$ (1 mM 4-AP)	−8.0 ± 0.1	5.6 ± 0.1
	Cav1.2+$\alpha_2\delta1$+Cav$\beta3$ (control)	−6.2 ± 0.1	6.1 ± 0.1
	Cav1.2+$\alpha_2\delta1$+Cav$\beta3$ (1 mM 4-AP)	−18.1 ± 0.1*	5.7 ± 0.1
N-type	Cav2.2+$\alpha_2\delta1$+Cav$\beta2$ (control)	−6.4 ± 0.1	4.8 ± 0.1
	Cav2.2+$\alpha_2\delta1$+Cav$\beta2$ (3 mM 4-AP)	−9.2 ± 0.1	4.6 ± 0.1
	Cav2.2+$\alpha_2\delta1$+Cav$\beta3$ (control)	−6.8 ± 0.1	4.8 ± 0.1
	Cav2.2+$\alpha_2\delta1$+Cav$\beta3$ (3 mM 4-AP)	−18.9 ± 0.1*	5.0 ± 0.1
P/Q-type	Cav2.1+$\alpha_2\delta1$+Cav$\beta2$ (control)	−8.1 ± 0.1	5.4 ± 0.1
	Cav2.1+$\alpha_2\delta1$+Cav$\beta2$ (3 mM 4-AP)	−8.1 ± 0.1	5.3 ± 0.1
	Cav2.1+$\alpha_2\delta1$+Cav$\beta3$ (control)	−6.7 ± 0.1	5.6 ± 0.1
	Cav2.1+$\alpha_2\delta1$+Cav$\beta3$ (3 mM 4-AP)	−8.1 ± 0.1	5.3 ± 0.1
Voltage-Dependent Inactivation			
L-type	Cav1.2+$\alpha_2\delta1$+Cav$\beta2$ (control)	−19.6 ± 0.3	−8.4 ± 0.2
	Cav1.2+$\alpha_2\delta1$+Cav$\beta2$ (1 mM 4-AP)	−18.7 ± 0.3	−8.4 ± 0.3
	Cav1.2+$\alpha_2\delta1$+Cav$\beta3$ (control)	−28.3 ± 0.3	−8.1 ± 0.3
	Cav1.2+$\alpha_2\delta1$+Cav$\beta3$ (1 mM 4-AP)	−28.2 ± 0.3	−8.2 ± 0.3
N-type	Cav2.2+$\alpha_2\delta1$+Cav$\beta2$ (control)	−24.8 ± 0.3	−7.8 ± 0.2
	Cav2.2+$\alpha_2\delta1$+Cav$\beta2$ (3 mM 4-AP)	−24.2 ± 0.3	−7.7 ± 0.3
	Cav2.2+$\alpha_2\delta1$+Cav$\beta3$ (control)	−51.2 ± 0.5	−7.9 ± 0.3
	Cav2.2+$\alpha_2\delta1$+Cav$\beta3$ (3 mM 4-AP)	−48.8 ± 0.4	−7.6 ± 0.3
P/Q-type	Cav2.1+$\alpha_2\delta1$+Cav$\beta2$ (control)	−20.2 ± 0.3	−9.1 ± 0.2
	Cav2.1+$\alpha_2\delta1$+Cav$\beta2$ (3 mM 4-AP)	−20.0 ± 0.3	−9.0 ± 0.3
	Cav2.1+$\alpha_2\delta1$+Cav$\beta3$ (control)	−23.4 ± 0.4	−9.3 ± 0.3
	Cav2.1+$\alpha_2\delta1$+Cav$\beta3$ (3 mM 4-AP)	−22.2 ± 0.3	−9.0 ± 0.4

*$P < 0.05$, compared with the respective control before 4-AP (paired Student's t test).

in either no or reduced basal whole-cell currents in HEK293 cells transfected with either Cav1.2 or Cav2.2 (Table 2), indicating that these residues are critical to Cavα_1-Cav$\beta3$ interactions or the function of Cav$\beta3$ and HVA Ca^{2+} channels. The A6 mutant had no basal whole-cell currents in Cav2.2-transfected HEK293 cells but had reduced basal Ba^{2+} currents in Cav2.1-transfected cells with an attenuated potentiating effect of 4-AP. In contrast, the A2 mutant resulted in wild-type–like basal whole-cell currents with either Cav1.2 or Cav2.2. Remarkably, the A2 mutation abolished the 4-AP potentiation of the L-type current and reduced the 4-AP effect on the N-type current to the level observed with Cav$\beta2$ (Fig. 7, A and B).

We next investigated whether other nonhomologous regions between Cav$\beta2$ and Cav$\beta3$ contribute to the distinct effect of

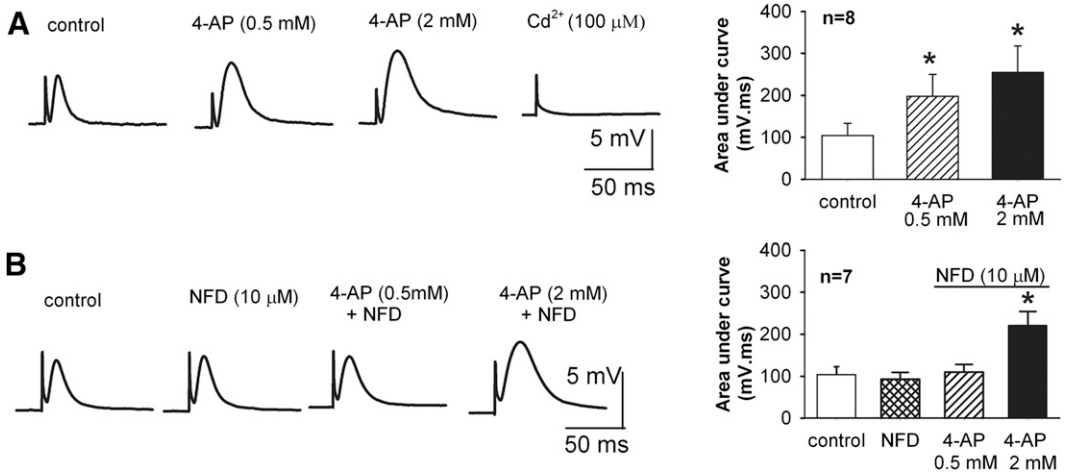

Fig. 3. N-type Ca^{2+} channels mediate the potentiating effect of low concentrations of 4-AP on neuromuscular transmission. (A) Original traces and summary data show the effect of 0.5 and 2 mM 4-AP on evoked EPPs in a rat phrenic nerve-diaphragm preparation (n = 8). (B) Representative recordings and group data show that blocking L-type Ca^{2+} channels with 10 μM nifedipine (NFD) blocked the effect of 0.5 mM 4-AP on EPPs. Note that 2 mM 4-AP still significantly augmented EPPs in the presence of nifedipine (n = 7). *$P < 0.05$ compared with the respective control (repeated measures analysis of variance followed by Dunnett's post hoc test).

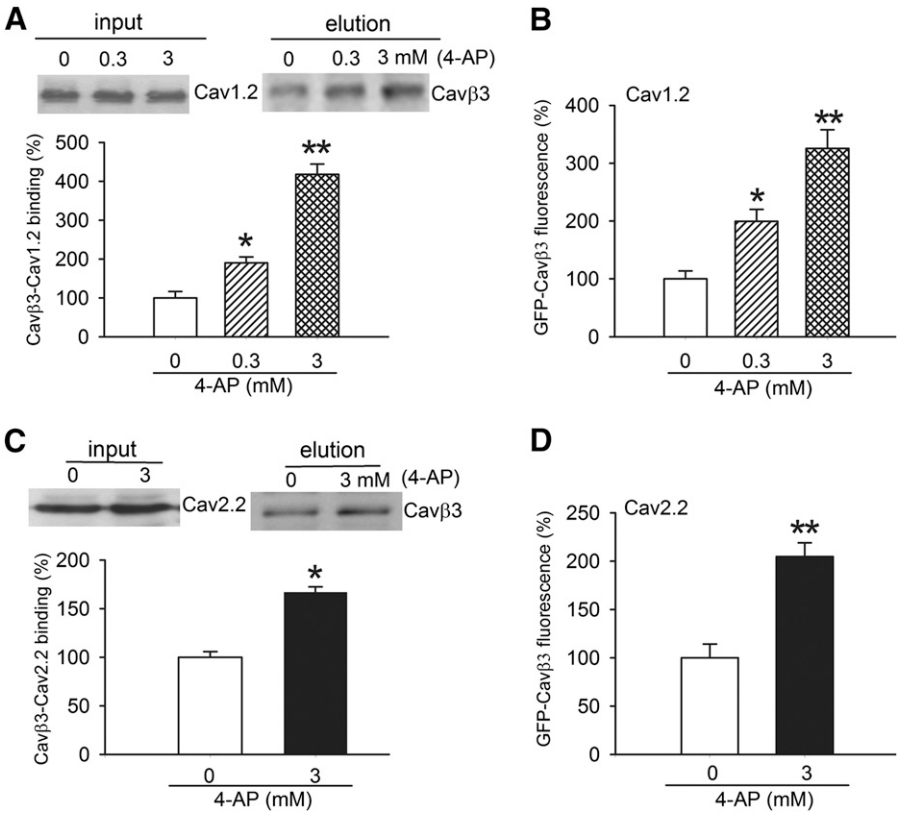

Fig. 4. 4-AP promotes the association of Cav1.2 and Cav2.2 to Cavβ3. (A and B) Original gel images and summary data show that 0.3 and 3 mM 4-AP increased the level of Cavβ3 proteins bound to Cav1.2 (A) and the amount of GFP-Cavβ3 protein retained with Cav1.2 (B). (C and D) Representative gel images and group data show the effect of 3 mM 4-AP on the levels of Cavβ3 protein bound to Cav2.2 (C) and the amount of GFP-Cavβ3 proteins retained with Cav2.2 measured using a fluorescence spectrophotometer (D). Data from 4-AP–treated samples were normalized to the control (without 4-AP). $N = 4$ separate transfection experiments in each group. $^*P < 0.05$, $^{**}P < 0.01$, compared with the control without 4-AP treatment (paired Student's t test or repeated measures analysis of variance followed by Dunnett's post hoc test).

4-AP on L-type and N-type Ca^{2+} channels. We aligned the amino acid sequences between Cavβ2 and Cavβ3 and used either domain swap or insertions to replace the different amino acid residues in Cavβ3 with the same amino acids in Cavβ2 at the equivalent positions. We generated four mutants in the HOOK and C-terminus domains of Cavβ3: P1 (K134 to G148), P2 (ins P367), P3 (ins G368), and P4 (ins E408) (Fig. 6). The Cavβ3 mutants were individually cotransfected with $\alpha_2\delta$1 and either Cav1.2 or Cav2.2. We then examined the basal whole-cell currents and effects of 4-AP on the N-type and L-type channels. Among the mutants in the C-terminus domain (P2–P4), P3 failed to produce any Ba^{2+} currents in HEK293 cells transfected with Cav1.2 and Cav2.2 (Fig. 7, A and B). In contrast, both the P2 and P4 Cavβ3 mutants generated wild-type–like Ba^{2+} currents. The P2 mutant had a significantly reduced 4-AP effect on both N-type and L-type currents to a level similar to that observed in cells transfected with Cavβ2. Interestingly, although insertion in the P4 mutant did not significantly alter the 4-AP effect on the N-type Ca^{2+} channel, it abolished the 4-AP effect on the L-type (Fig. 7, A and B; Table 2).

The P1 mutant in the HOOK region of Cavβ3 produced wild-type–like N-type and L-type currents. Remarkably, the potentiating effect of 4-AP on both N-type and L-type Ca^{2+} channels expressed in HEK293 cells carrying P1 mutant was dramatically decreased to a level similar to that in cells cotransfected with Cavβ2 (Fig. 7, A and B). We further divided the P1 domain into four smaller pieces and individually mutated residues in each to alanines (Fig. 6). Among these mutants, the P1a (K134 to R137) mutant produced no N-type currents although it produced wild-type–like L-type currents with diminished 4-AP effect. The P1b (S138 to P141) mutant either generated no currents or reduced basal N-type and L-type currents (Table 2). The P1c (S142 to S145) mutant did not produce any measurable L-type currents but generated wild-type–like N-type currents. The potentiating effect of 4-AP on N-type currents was not altered in HEK293 cells coexpressing the P1c mutant. Interestingly, P1d (D146 to G148) generated wild-type–like N-type and L-type currents but with a significantly reduced 4-AP potentiating effect, recapitulating the effect of the P1 (K134 to G148) mutant (Fig. 7, A–D). Also, Cavβ3-P1d significantly attenuated the 4-AP–mediated hyperpolarizing shift in voltage-dependent activation of L-type and N-type Ca^{2+} channels compared with that in the wild-type Cavβ3 control (Fig. 7E).

We further mutated D146, I147, and G148 to alanine and determined the 4-AP effect on L-type and N-type currents. Among these mutants, P1-D146A generated wild-type–like L-type and N-type currents, but with a diminished 4-AP effect for L-type currents. P1-I147 and P1-G148 generated wild-type–like L-type currents but did not produce any measurable N-type currents. Interestingly, the potentiating effect of 4-AP on L-type currents was diminished with P1-I147, but not with P1-G148, mutant (Fig. 7, A and B; Table 2). Concentration-response relationships of 4-AP on the L-type Ca^{2+} channel with P1d (D146-G148) and P1-D146 were similar to those of a single concentration of 4-AP (Fig. 7D). Taken together, these results indicate that residues in P1d in the HOOK domain, A2 in the GK domain, and P2 in the C-terminus domain of Cavβ3 are critical determinants for the 4-AP–mediated potentiation of L-type and N-type Ca^{2+} channels.

Discussion

A major finding of our study is that L-type Ca^{2+} channels are a probable therapeutic target of 4-AP for the treatment of

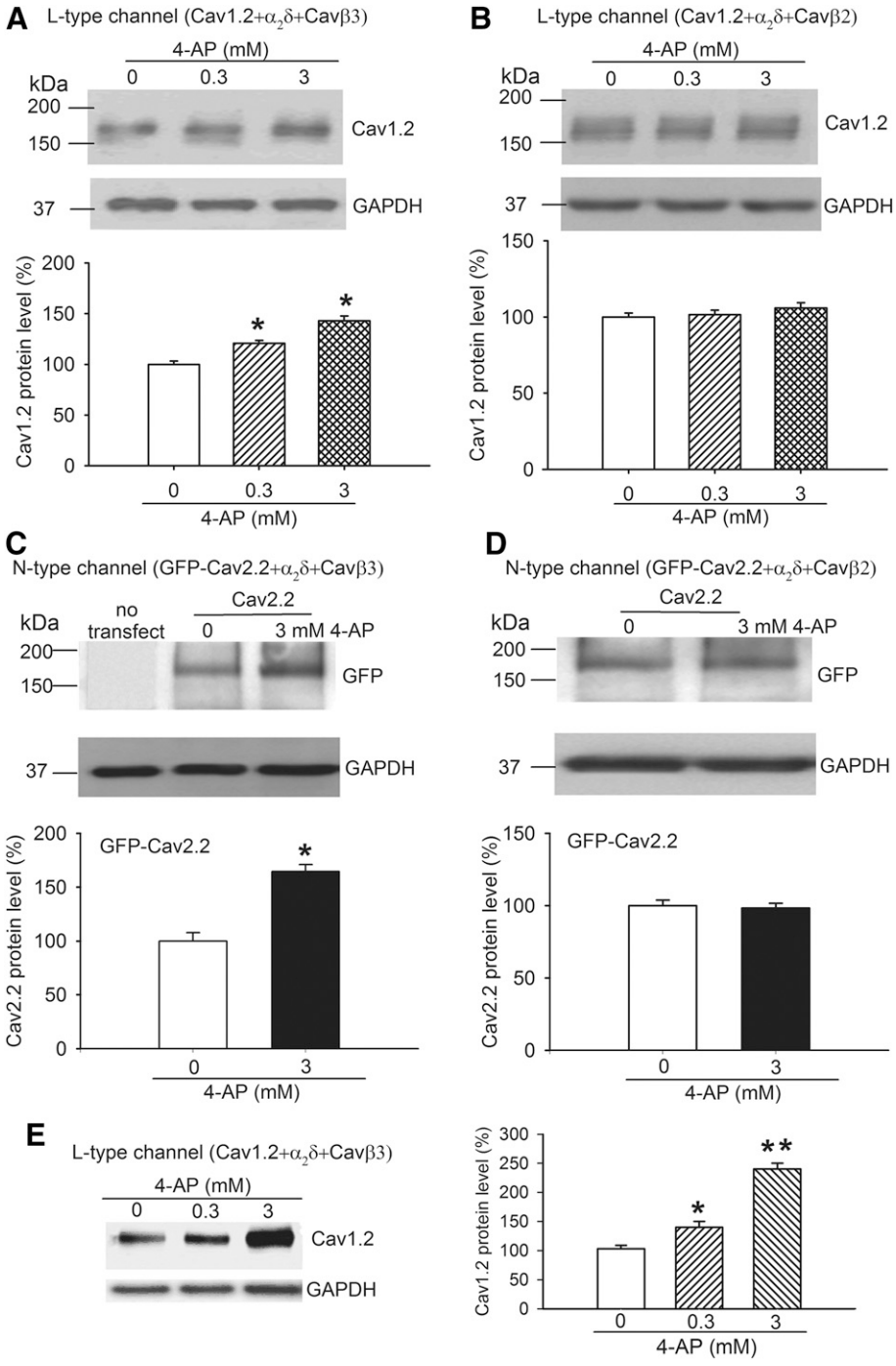

Fig. 5. 4-AP acts through Cavβ3 to increase the plasma membrane expression of Cav1.2 and Cav2.2. (A and B) Original gel images and group data show the differential effect of 0.3 and 3 mM 4-AP on the protein level of Cav1.2 on the plasma membrane in HEK293 cells transfected with $\alpha_2\delta$1 and either Cavβ3 (A) or Cavβ2 (B). (C and D) Representative gel images and summary data illustrate the differential effect of 3 mM 4-AP on the protein level of Cav2.2 on the plasma membrane in cells cotransfected with $\alpha_2\delta$1 and either Cavβ3 (C) or Cavβ2 (D). N = 4 separate experiments in each group. (E) Original gel image and mean data show the effect of 0.3 and 3 mM 4-AP on the protein level of Cav1.2 on the plasma membrane surface in HEK293 cells cotransfected with $\alpha 2\delta 1$ and Cavβ3 (N = 5 separate experiments in each group). Data from 4-AP–treated samples were first normalized by using the loading (GAPDH) control and then normalized to the control group (without 4-AP). $^*P < 0.05$, $^{**}P < 0.01$, compared with the control without 4-AP (paired Student's t test or repeated measures analysis of variance followed by Dunnett's post hoc test).

impaired neuromuscular function. We have recently demonstrated that at millimolar concentrations, 4-AP can directly stimulate N-type Ca^{2+} channels through a coexpressed Cavβ3 subunit (Wu et al., 2009). However, the millimolar concentration of 4-AP required to potentiate native and recombinant N-type Ca^{2+} channels does not match well with the micromolar concentration of 4-AP needed to increase neuromuscular transmission. We thus systematically investigated the potential roles of other Cavβ subunits in the effects of 4-AP on different subtypes of HVA Ca^{2+} channels reconstituted in HEK293 cells. In the present study, we found that 4-AP significantly increased N-type currents at 3 mM but had little effect on P/Q-type currents up to 10 mM. Unexpectedly, 4-AP at micromolar concentrations largely potentiated Cav1.2 L-type currents. This finding is potentially highly significant because only micromolar concentrations of 4-AP are relevant to the therapeutic effects of 4-AP in patients (Bever et al., 1994; Smith et al., 2000). Both N-type and L-type Ca^{2+} channels are present in presynaptic terminals at neuromuscular junctions (Thaler et al., 2001; Perissinotti et al., 2008). Cav1.2 is widely expressed in the heart, pancreas, adrenal gland, and nervous system (Snutch et al., 1991; Dirksen and Beam, 1996). It has been shown that Cav1.2 is located both pre- and postsynaptically in the brain (Tippens et al., 2008) and is present on peripheral nerve axons (Enes et al., 2010).

Fig. 6. Mutagenesis studies in the SH3, HOOK, GK and C-terminus (CT) domains of Cavβ3 subunit. Amino acid sequence alignment of Cavβ1–4 subunits highlights the regions and amino acid residues selected for mutagenesis (marked with blue boxes). Amino acid residues marked in red are those involved in interactions with AID in Cavα_1 subunits.

Interestingly, nifedipine had no effect on EPPs before 4-AP application, suggesting that non–L-type Ca^{2+} channels are essential for evoked acetylcholine release at the neuromuscular junction (Lin and Lin-Shiau, 1997; Oliveira et al., 2004). We found that blocking L-type channels with nifedipine blocked the potentiating effect of low concentrations of 4-AP on EPPs in a neuromuscular junction preparation. This is consistent with our finding that micromolar concentrations of 4-AP only increased L-type currents reconstituted with Cav1.2-Cavβ3 in HEK293 cells. Our data indicate that the "silent" L-type channels play a major role in the stimulatory effect of 4-AP at the neuromuscular junction. Cav1.2 is the most abundant neuronal L-type Ca^{2+} channel (Hell et al., 1993; Bourinet et al., 1994). However, we cannot exclude the possibility that Cav1.3 may be also involved in the potentiating effect of 4-AP on neuromuscular transmission. Because 4-AP blocks voltage-activated K^+ channels only at millimolar concentrations (Wu et al., 2009), our study provides further evidence that 4-AP–induced increases in Ca^{2+} influx and neurotransmitter release in various experimental preparations are predominantly through its direct stimulating effect on HVA Ca^{2+} channels. In addition, 4-AP has been used to effectively treat patients who have overdosed on L-type Ca^{2+} channel blockers (ter Wee et al., 1985; Hofer et al., 1993; Wilffert et al., 2007). Our study thus provides a novel mechanistic basis for using 4-AP as an antidote to treat the overdose symptoms of L-type Ca^{2+} channel blockers.

Another intriguing finding of our study is that potentiation of HVA Ca^{2+} channels by 4-AP is highly dependent on the nature of the Cavβ subunit and that at least for the Cav1.2 L-type Ca^{2+} channel, Cavβ3 is the only Cavβ subunit capable of mediating the 4-AP potentiating effect. We found that 4-AP increased N-type and L-type currents mainly through Cavβ3, but not Cavβ2. In the presence of the same Cavα_1 and $\alpha_2\delta$1 subunits, 0.1–1 mM 4-AP largely potentiated L-type Ca^{2+} channels almost exclusively through Cavβ3. In contrast, for N-type Ca^{2+} channels, Cavβ3 and Cavβ4 seem to play an equally important role in the effect of 4-AP. For P/Q-type channels, 4-AP failed to affect their currents regardless of the Cavβ subunit cotransfected. These findings suggest that the structural and/or conformational differences in the interactions between Cavα_1 and Cavβ3 determine the differential effect of 4-AP on N-type and L-type Ca^{2+} channels. The Cavβ3 subunit is strongly expressed in the smooth muscle, heart, and central and peripheral nervous systems, and it complexes with ~40% of brain L-type Ca^{2+} channels (Ludwig et al., 1997; Namkung et al., 1998; Li et al., 2012). Interestingly, nerve injury can upregulate Cavβ3 expression (Li et al., 2012), and this upregulation may further augment the 4-AP effect on L-type Ca^{2+} channels and neurotransmitter release from damaged nerve terminals.

Our results obtained from both plasma membrane extraction and biotinylation assays strongly suggest that 4-AP may

TABLE 2

Effects of Cavβ3 mutations on 4-AP–induced potentiation of N-type and L-type Ca^{2+} channels in HEK293 cells

n = 6–8 cells in each group; data are expressed as means ± S.E.M.

Mutant	Mutation Sites	N-type		L-type		
		% Increase in I_{Ba} (3 mM 4-AP)	Basal I_{Ba}	% Increase in I_{Ba} (0.3 mM 4-AP)	% Increase in I_{Ba} (1 mM 4-AP)	Basal I_{Ba}
			pA			*pA*
Cavβ3 (wild-type)		183.9 ± 34.4%	786.5 ± 180.2	122.5 ± 22.4%	250.5 ± 20.8%	389.1 ± 91.5
Cavβ2 (wild-type)		77.7 ± 22.9%	748.1 ± 51.8	11.1 ± 3.8%	46.6 ± 21.4%	333.4 ± 13.8
Cavβ3-A1 (M195-M196)	MM → AA	No effect	15.8 ± 8.4 **	50.7 ± 5.5% *	52.5 ± 8.6% *	45.5 ± 13.9 **
Cavβ3-A2 (K198-L200)	KAL→ AGA	99.8 ± 15.8% *	651.7 ± 110.4	No effect	No effect	645.8 ± 93.0
Cavβ3-A3 (V292-S295)	VKVS → AKAA	No currents	No currents	No currents	No currents	No currents
Cavβ3-A4 (V299-L303)	VLQRL → ALQAA	No effect	33.3 ± 13.1 **	No currents	No currents	No currents
Cavβ3-A5 (L337-N340)	LDEN → ADAA	66.2 ± 10.5% *	42.8 ± 9.2 **	No currents	No currents	No currents
Cavβ3-A6 (L342-A345)	LDDA → ADDG	No currents	No currents	5.13 ± 2.5% **	23.8 ± 4.6% **	248.2 ± 198.7
Cavβ3-P1 (K134-G148)	KARRSGNPSSLSDIG (Cavβ3) →RAKQGKFYSSKSGGNSSSSLGDIVPS (Cavβ2)	71.9 ± 19.6% *	661.8 ± 137.9	15.6 ± 5.6% **	54.9 ± 3.5% *	583.3 ± 210.4
Cavβ3-P1a (K134-R137)	KARR → AAAA	No currents	No currents	No effect	No effect	316.5 ± 93.4
Cavβ3-P1b (S138-P141)	SGNP → AAAA	18.3 ± 5.1% **	138.2 ± 37.9 **	No currents	No currents	No currents
Cavβ3-P1c (S142-S145)	SSLS → AAAA	214.5 ± 50.6%	690.8 ± 93.0	No currents	No currents	No currents
Cavβ3-P1d (D146-G148)	DIG → AAA	45.8 ± 31.3% *	722.1 ± 110.5	14.0 ± 2.8% **	52.8 ± 23.5% *	289.4 ± 140.4
Cavβ3-P1-D146	D → A	167.2 ± 35.4%	628.8 ± 125.5	15.0 ± 3.5% **	52.5 ± 11.3% *	245.1 ± 58.9
Cavβ3-P1-I147	I → A	No currents	No currents	55.2 ± 20.8% *	64.1 ± 3.5% *	307.7 ± 76.2
Cavβ3-P1-G148	G → A	No currents	No currents	4.17 ± 1.5% **	193.7 ± 2.9%	222.8 ± 88.7
Cavβ3-P2 (ins P367)	(ins) PNPLLSRT (Cavβ2)	60.2 ± 8.3% *	750.8 ± 131.8	20.8 ± 11.3% **	78.3 ± 2.3% *	625.9 ± 97.5
Cavβ3-P3 (ins G368)	(ins) ATST (Cavβ2)	No currents	No currents	No currents	No currents	No currents
Cavβ3-P4 (ins E480)	(ins) PVKKSQHRSSSATH (Cavβ2)	148.9 ± 20.5%	850.4 ± 179.2	No effect	No effect	598.6 ± 154.3

*$P < 0.05$, **$P < 0.01$, compared with the Cavβ3 wide-type controls (repeated measures analysis of variance followed by Dunnett's post hoc test).

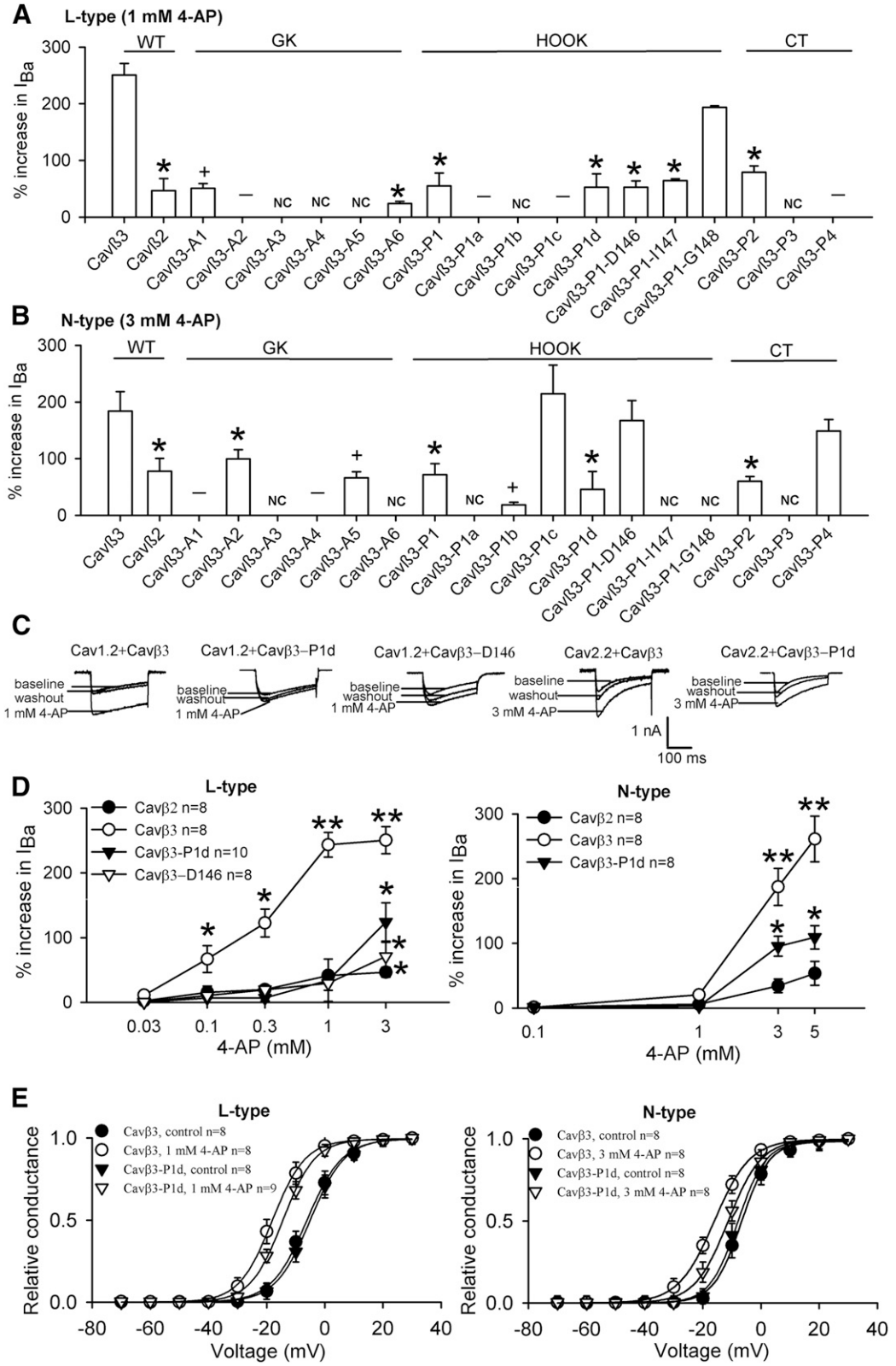

Fig. 7. Residues in the GK, HOOK, and C-terminus domains critically determine the potentiating effect of 4-AP on N-type and L-type Ca^{2+} channels. (A and B) Summary data show the distinct effects of 4-AP on L-type [Cav1.2, (A)] and N-type [Cav2.2, (B)] currents in HEK293 cells reconstituted with $\alpha_2\delta1$ and various Cavβ3 mutants (n = 6–8 cells in each group). (C and D) Original current traces and group data show that the potentiating effects of 4-AP on L-type and N-type currents were reduced in cells transfected with Cavβ3-P1d or Cavβ3-P1-D146. NC denotes no Ba^{2+} currents; – designates no 4-AP effects; + denotes reduced basal Ba^{2+} currents. (E) Effects of 4-AP on the voltage-dependent activation of L-type and N-type Ca^{2+} channels in HEK293 cells transfected with wild-type Cavβ3 or Cavβ3-P1d mutant. The hyperpolarizing shift in the voltage-dependence of activation of L-type and N-type Ca^{2+} channels by 4-AP was attenuated in cells cotransfected with Cavβ3-P1d, compared with that for the wild-type Cavβ3. $^*P < 0.05$, $^{**}P < 0.01$ compared with the baseline control or wild-type Cavβ3 control (repeated measures analysis of variance followed by Dunnett's post hoc test).

act to increase the association between Cavβ3 and Cav1.2 and Cav2.2 subunits, leading to increased trafficking of Cav1.2 and Cav2.2 to the cell membrane surface. Cavβ subunits appear to regulate HVA Ca^{2+} channel function by promoting Cavα_1 surface expression, protecting against degradation, and affecting voltage-dependent, kinetic, and modulatory characteristics (De Waard et al., 1994; Pragnell et al., 1994; Stea et al., 1994; Bourinet et al., 1996; Yamaguchi et al., 1998; Altier et al., 2011; Waithe et al., 2011; Dolphin, 2012). In the present study, we found that 4-AP significantly shifted voltage-dependent activation of L-type and N-type Ca^{2+} channels, consistent with the known functions of Cavβ subunits. Moreover, our biochemical assays revealed that 4-AP at concentrations that effectively increase N-type and L-type currents profoundly increased the amount of Cavβ3 proteins bound to the Cav1.2 and Cav2.2 subunits and promoted the expression of Cavα_1 on the plasma membrane. These effects on membrane trafficking were specific to the selective Cavβ3 subunit, because we did not observe any effect when Cavβ3 was replaced with Cavβ2. These 4-AP effects provide additional evidence that the intracellular Cavβ3 subunit plays an important role in regulating Cavα_1 trafficking and HVA Ca^{2+} channel functions. Although we found that Cavβ3-dependent trafficking occurred within a few minutes after 4-AP application, it is not clear to what extent this action contributes to the rapid potentiation of Ca^{2+} channel activity by 4-AP. The actions of 4-AP on both channel activation and trafficking may contribute to the potentiating effects of 4-AP on N-type and L-type channels. However, the potential effects of 4-AP on the subcellular distribution of Ca^{2+} channels are not clear and warrant further studies.

The SH3-HOOK-GK module is the core structure of the Cavβ subunit and dictates the function of the Cavβ subunit (Chen et al., 2004; Buraei and Yang, 2010; Dolphin, 2012). In our mutagenesis experiments, we specifically sought to identify residues that do not affect the basal activity of HVA Ca^{2+} channels, but do diminish the potentiating effect of 4-AP. Our analyses revealed that several protein domains in the GK (A2), HOOK (P1-day), and C-terminus (P2) regions of Cavβ3 are major determinants of the potentiating effect of 4-AP on L-type and N-type currents. These findings suggest that 4-AP might act through specific regions in concert to alter the folding and/or structure of Cavβ3 to augment its interaction with certain Cavα_1 subunits. Interestingly, mutating several residues (e.g., A2, P1c, P1-D146, and P4) in the GK, HOOK, and C-terminus domains generally blocked the 4-AP effect more in L-type than in N-type Ca^{2+} channels, which may explain the distinct sensitivity of these two channels to 4-AP. It has been shown that the AID site, a highly conserved intracellular region within the domain I-II linker of HVA Cavα_1 subunits, is the principal domain that interacts with Cavβ subunits (Pragnell et al., 1994; Bichet et al., 2000; Bourdin et al., 2010). The GK domain of Cavβ subunits binds with high affinity to the AID site in Cavα_1 (Chen et al., 2004; Opatowsky et al., 2004; Van Petegem et al., 2004). 4-AP may also induce interactions between several residues in the HOOK and C-terminus domains of Cavβ3 and Cavα_1. Conformational changes of these sites induced by 4-AP might substantially increase the binding of Cavβ3 to Cavα_1. Alternatively, because the SH3-GK intramolecular interaction is important for the function of Cavβ (McGee et al., 2004; Takahashi et al., 2005; Chen et al., 2009), 4-AP may promote Cavβ3-AID binding by strengthening the SH3-GK intramolecular interaction. Our results suggest that the dynamic association between Cavβ3 and Cavα_1 plays a critical role in the 4-AP potentiation of HVA Ca^{2+} channels. Thus, 4-AP may prove to be a valuable tool in determining any postulated conformational/binding changes relevant to Cavβ3 interaction with Cavα_1 subunits and other partners.

In summary, our findings from this study provide substantial new evidence that the potentiating effect of 4-AP on HVA Ca^{2+} channels critically depends on the specific combinations of Cavα_1 and Cavβ subunits. Of particular note, 4-AP at micromolar concentrations selectively stimulates L-type Ca^{2+} channels in the presence of Cavβ3 by increasing Cav1.2-Cavβ3 physical interaction and surface expression. Residues in both conserved and variable domains of the Cavβ3 subunit are critically involved in the 4-AP potentiation of L-type and N-type Ca^{2+} channels. This new information is important not only to understanding the molecular mechanisms underlying 4-AP actions on HVA Ca^{2+} channels but also to designing improved strategies to treat patients with impaired neuromuscular function.

Acknowledgments

The authors thank Drs. Diane Lipscombe, Terrance P. Snutch, and Tsutomu Tanabe for providing the Ca^{2+} channel subunit cDNAs used in our study.

Authorship Contributions

Participated in research design: L. Li, D.-P. Li, S.-R. Chen, Hu, Pan.
Conducted experiments: L. Li, D.-P. Li, J. Chen, S.-R. Chen.
Performed data analysis: L. Li, D.-P. Li, J. Chen, S.-R. Chen, Hu, Pan.
Wrote or contributed to the writing of the manuscript: L. Li, Pan.

References

Altier C, Garcia-Caballero A, Simms B, You H, Chen L, Walcher J, Tedford HW, Hermosilla T, and Zamponi GW (2011) The Cavβ subunit prevents RFP2-mediated ubiquitination and proteasomal degradation of L-type channels. *Nat Neurosci* **14**: 173–180.

Bever CT, Jr, Young D, Anderson PA, Krumholz A, Conway K, Leslie J, Eddington N, Plaisance KI, Panitch HS, and Dhib-Jalbut S et al. (1994) The effects of 4-aminopyridine in multiple sclerosis patients: results of a randomized, placebo-controlled, double-blind, concentration-controlled, crossover trial. *Neurology* **44**:1054–1059.

Bichet D, Lecomte C, Sabatier JM, Felix R, and De Waard M (2000) Reversibility of the Ca(2+) channel alpha(1)-beta subunit interaction. *Biochem Biophys Res Commun* **277**:729–735.

Bourdin B, Marger F, Wall-Lacelle S, Schneider T, Klein H, Sauvé R, and Parent L (2010) Molecular determinants of the CaVbeta-induced plasma membrane targeting of the CaV1.2 channel. *J Biol Chem* **285**:22853–22863.

Bourinet E, Charnet P, Tomlinson WJ, Stea A, Snutch TP, and Nargeot J (1994) Voltage-dependent facilitation of a neuronal alpha 1C L-type calcium channel. *EMBO J* **13**:5032–5039.

Bourinet E, Soong TW, Stea A, and Snutch TP (1996) Determinants of the G protein-dependent opioid modulation of neuronal calcium channels. *Proc Natl Acad Sci USA* **93**:1486–1491.

Buraei Z and Yang J (2010) The ß subunit of voltage-gated Ca2+ channels. *Physiol Rev* **90**:1461–1506.

Catterall WA (2000) Structure and regulation of voltage-gated Ca2+ channels. *Annu Rev Cell Dev Biol* **16**:521–555.

Catterall WA and Few AP (2008) Calcium channel regulation and presynaptic plasticity. *Neuron* **59**:882–901.

Catterall WA, Perez-Reyes E, Snutch TP, and Striessnig J (2005) International Union of Pharmacology. XLVIII. Nomenclature and structure-function relationships of voltage-gated calcium channels. *Pharmacol Rev* **57**:411–425.

Chen YH, Li MH, Zhang Y, He LL, Yamada Y, Fitzmaurice A, Shen Y, Zhang H, Tong L, and Yang J (2004) Structural basis of the alpha1-beta subunit interaction of voltage-gated Ca2+ channels. *Nature* **429**:675–680.

Chen YH, He LL, Buchanan DR, Zhang Y, Fitzmaurice A, and Yang J (2009) Functional dissection of the intramolecular Src homology 3-guanylate kinase domain coupling in voltage-gated Ca2+ channel beta-subunits. *FEBS Lett* **583**:1969–1975.

Davis FA, Stefoski D, and Rush J (1990) Orally administered 4-aminopyridine improves clinical signs in multiple sclerosis. *Ann Neurol* **27**:186–192.

De Waard M, Pragnell M, and Campbell KP (1994) Ca2+ channel regulation by a conserved beta subunit domain. *Neuron* **13**:495–503.

Dirksen RT and Beam KG (1996) Unitary behavior of skeletal, cardiac, and chimeric L-type Ca2+ channels expressed in dysgenic myotubes. *J Gen Physiol* **107**:731–742.

Dolphin AC (2012) Calcium channel auxiliary α2δ and β subunits: trafficking and one step beyond. *Nat Rev Neurosci* **13**:542–555.

Enes J, Langwieser N, Ruschel J, Carballosa-Gonzalez MM, Klug A, Traut MH, Ylera B, Tahirovic S, Hofmann F, and Stein V et al. (2010) Electrical activity suppresses

axon growth through Ca(v)1.2 channels in adult primary sensory neurons. *Curr Biol* **20**:1154–1164.
Giovannini F, Sher E, Webster R, Boot J, and Lang B (2002) Calcium channel subtypes contributing to acetylcholine release from normal, 4-aminopyridine-treated and myasthenic syndrome auto-antibodies-affected neuromuscular junctions. *Br J Pharmacol* **136**:1135–1145.
Hansebout RR, Blight AR, Fawcett S, and Reddy K (1993) 4-Aminopyridine in chronic spinal cord injury: a controlled, double-blind, crossover study in eight patients. *J Neurotrauma* **10**:1–18.
Hell JW, Westenbroek RE, Warner C, Ahlijanian MK, Prystay W, Gilbert MM, Snutch TP, and Catterall WA (1993) Identification and differential subcellular localization of the neuronal class C and class D L-type calcium channel alpha 1 subunits. *J Cell Biol* **123**:949–962.
Hidalgo P, Gonzalez-Gutierrez G, Garcia-Olivares J, and Neely A (2006) The alpha1-beta-subunit interaction that modulates calcium channel activity is reversible and requires a competent alpha-interaction domain. *J Biol Chem* **281**:24104–24110.
Hofer CA, Smith JK, and Tenholder MF (1993) Verapamil intoxication: a literature review of overdoses and discussion of therapeutic options. *Am J Med* **95**:431–438.
Kim YI and Neher E (1988) IgG from patients with Lambert-Eaton syndrome blocks voltage-dependent calcium channels. *Science* **239**:405–408.
Li L, Cao XH, Chen SR, Han HD, Lopez-Berestein G, Sood AK, and Pan HL (2012) Up-regulation of Cavβ3 subunit in primary sensory neurons increases voltage-activated Ca2+ channel activity and nociceptive input in neuropathic pain. *J Biol Chem* **287**:6002–6013.
Lin MJ and Lin-Shiau SY (1997) Multiple types of Ca2+ channels in mouse motor nerve terminals. *Eur J Neurosci* **9**:817–823.
Ludwig A, Flockerzi V, and Hofmann F (1997) Regional expression and cellular localization of the alpha1 and beta subunit of high voltage-activated calcium channels in rat brain. *J Neurosci* **17**:1339–1349.
Lundh H, Nilsson O, and Rosén I (1979) Effects of 4-aminopyridine in myasthenia gravis. *J Neurol Neurosurg Psychiatry* **42**:171–175.
McGee AW, Nunziato DA, Maltez JM, Prehoda KE, Pitt GS, and Bredt DS (2004) Calcium channel function regulated by the SH3-GK module in beta subunits. *Neuron* **42**:89–99.
Namkung Y, Smith SM, Lee SB, Skrypnyk NV, Kim HL, Chin H, Scheller RH, Tsien RW, and Shin HS (1998) Targeted disruption of the Ca2+ channel beta3 subunit reduces N- and L-type Ca2+ channel activity and alters the voltage-dependent activation of P/Q-type Ca2+ channels in neurons. *Proc Natl Acad Sci USA* **95**:12010–12015.
Oliveira L, Timóteo MA, and Correia-de-Sá P (2004) Tetanic depression is overcome by tonic adenosine A(2A) receptor facilitation of L-type Ca(2+) influx into rat motor nerve terminals. *J Physiol* **560**:157–168.
Opatowsky Y, Chen CC, Campbell KP, and Hirsch JA (2004) Structural analysis of the voltage-dependent calcium channel beta subunit functional core and its complex with the alpha 1 interaction domain. *Neuron* **42**:387–399.
Perissinotti PP, Giugovaz Tropper B, and Uchitel OD (2008) L-type calcium channels are involved in fast endocytosis at the mouse neuromuscular junction. *Eur J Neurosci* **27**:1333–1344.
Pragnell M, De Waard M, Mori Y, Tanabe T, Snutch TP, and Campbell KP (1994) Calcium channel beta-subunit binds to a conserved motif in the I-II cytoplasmic linker of the alpha 1-subunit. *Nature* **368**:67–70.
Smith KJ, Felts PA, and John GR (2000) Effects of 4-aminopyridine on demyelinated axons, synapses and muscle tension. *Brain* **123**:171–184.
Snutch TP, Tomlinson WJ, Leonard JP, and Gilbert MM (1991) Distinct calcium channels are generated by alternative splicing and are differentially expressed in the mammalian CNS. *Neuron* **7**:45–57.
Stea A, Tomlinson WJ, Soong TW, Bourinet E, Dubel SJ, Vincent SR, and Snutch TP (1994) Localization and functional properties of a rat brain alpha 1A calcium channel reflect similarities to neuronal Q- and P-type channels. *Proc Natl Acad Sci USA* **91**:10576–10580.
Stea A, Soong TW, and Snutch TP (1995) Determinants of PKC-dependent modulation of a family of neuronal calcium channels. *Neuron* **15**:929–940.
Strupp M, Kalla R, Dichgans M, Freilinger T, Glasauer S, and Brandt T (2004) Treatment of episodic ataxia type 2 with the potassium channel blocker 4-aminopyridine. *Neurology* **62**:1623–1625.
Takahashi SX, Miriyala J, Tay LH, Yue DT, and Colecraft HM (2005) A CaVbeta SH3/guanylate kinase domain interaction regulates multiple properties of voltage-gated Ca2+ channels. *J Gen Physiol* **126**:365–377.
ter Wee PM, Kremer Hovinga TK, Uges DR, and van der Geest S (1985) 4-Aminopyridine and haemodialysis in the treatment of verapamil intoxication. *Hum Toxicol* **4**: 327–329.
Thaler C, Li W, and Brehm P (2001) Calcium channel isoforms underlying synaptic transmission at embryonic Xenopus neuromuscular junctions. *J Neurosci* **21**: 412–422.
Tippens AL, Pare JF, Langwieser N, Moosmang S, Milner TA, Smith Y, and Lee A (2008) Ultrastructural evidence for pre- and postsynaptic localization of Cav1.2 L-type Ca2+ channels in the rat hippocampus. *J Comp Neurol* **506**: 569–583.
Van Petegem F, Clark KA, Chatelain FC, and Minor DL, Jr (2004) Structure of a complex between a voltage-gated calcium channel beta-subunit and an alpha-subunit domain. *Nature* **429**:671–675.
Waithe D, Ferron L, Page KM, Chaggar K, and Dolphin AC (2011) Beta-subunits promote the expression of Ca(V)2.2 channels by reducing their proteasomal degradation. *J Biol Chem* **286**:9598–9611.
Wilffert B, Boskma RJ, van der Voort PH, Uges DR, van Roon EN, and Brouwers JR (2007) 4-Aminopyridine (fampridine) effectively treats amlodipine poisoning: a case report. *J Clin Pharm Ther* **32**:655–657.
Wu ZZ, Li DP, Chen SR, and Pan HL (2009) Aminopyridines potentiate synaptic and neuromuscular transmission by targeting the voltage-activated calcium channel beta subunit. *J Biol Chem* **284**:36453–36461.
Yamaguchi H, Hara M, Strobeck M, Fukasawa K, Schwartz A, and Varadi G (1998) Multiple modulation pathways of calcium channel activity by a beta subunit. Direct evidence of beta subunit participation in membrane trafficking of the alpha1C subunit. *J Biol Chem* **273**:19348–19356.

Address correspondence to: Dr. Hui-Lin Pan, Department of Anesthesiology and Perioperative Medicine, Unit 110, The University of Texas MD Anderson Cancer Center, 1515 Holcombe Blvd., Houston, TX 77030. E-mail: huilinpan@mdanderson.org